Environment and Ecology 39 (2) : 323—331, April—June 2021
ISSN 0970-0420

# Comparison of Surface Albedo and Normalized Difference Vegetation Index for Different Land Use/Cover

**J. Ramachandran, R. Lalitha, S. Vallal Kannan, K. Sivasubramanian**

Received 12 October 2020, Accepted 26 February 2021, Published on 7 April 2021

## ABSTRACT

The objective of this paper is to compute surface albedo and Normalized Difference Vegetation Index (NDVI) from Landsat 8 satellite images for different land use/cover in Lalgudi block, Tiruchirapalli District, Tamil Nadu, India. Two pairs (December 2014 and January 2015 and December 2017 and January 2018) of Landsat 8 satellite images were used in this study. Results indicated that, surface albedo values for sand bed, water body, barren land, vegetation and settlements varied between 0.2 to 0.37, 0.05 to 0.10, 0.2 to 0.3, 0.15 to 0.20 and 0.12 to 0.23 respectively. NDVI values varied between 0.1 to 0.3 for settlements, 0.3 to 0.5 for vegetation and -0.07 to -0.09 for water bodies. The surface albedo values provided higher degree of differentiation for land use/cover when compared to NDVI. Correlation coefficient was estimated between Surface Albedo-NDVI that resulted in negative value (-0.3). An inverse relation between Surface Albedo-NDVI was revealed. Ground control points of different land use/cover were chosen by making field visits. The variation of two parameters were compared graphically for each land use/cover. Overall, making use of surface albedo and NDVI could improve differentiation of land use/cover.

**Keywords** Surface Albedo, NDVI, Landsat 8, Land use/cover.

J. Ramachandran*,
Teaching Assistant, Department of Agricultural Engineering, AC&RI, TNAU, Madurai 625002, India

R. Lalitha
Professor (SWCE) and Head, Department of SWCE, AEC&RI, TNAU, Kumulur, Trichy 621712, India

S. Vallal Kannan
Assistant Professor (Agronomy), Department of IDE, AEC&RI, TNAU, Kumulur, Trichy 621712, India

K. Sivasubramanian
Associate Professor (Environmental Sciences), Office of CoE, TNAU, Coimbatore 641003, India
Email: ecesurgstnuae@gmail.com
*Corresponding author

## INTRODUCTION

Land use/cover mapping is done through field surveys which is laborious, time consuming and does not capture the spatial changes in land use/cover types. Remote sensing with multi-spectral high-resolution satellite data acts as a strong tool in monitoring aspects of land use/cover changes. The accuracy of land use/cover classification depends on method or index used for classification.

Surface albedo is an important climate variable. It is the proportion of solar energy reflected back by the earth's surface and used in calculation of earth's surface energy (Liaqat and Choi 2015) and water balance studies (Semmens *et al.* 2016). NDVI is the ratio of differences between reflectivity of near-infrared and red band to their sum. It specifies the condition of the vegetation most accurately. Most commonly, both the indexes are used for performing land use/cover classification.

Landsat 8 is a science mission satellite that carries two sensors namely: Operational Land Imager (OLI) and Thermal Infrared Sensor (TIRS). This incorporates improved performance of Landsat 8 over the other Landsat missions (Roy *et al.* 2014).Surface albedo cannot be directly obtained from the Landsat 8 image. da Silva *et al*. (2016) presented an elaborate procedure for computing surface albedo from OLI images. Due to increased radiometric resolution of sensors in Landsat 8, the surface albedo obtained with OLI images provides more significant degree of differentiation in land use/cover classification (da Silva *et al.* 2016). Yao *et al*. (2008) explored the relationship between the surface albedo-NDVI using the Landsat 7 ETM + data products. Salifu and Agyare (2012) estimated surface albedo and NDVI for distinguishing land use/cover types.

In this study, from OLI-TIRS Landsat 8 data products, surface albedo and NDV Iwere computed. This study was conducted in Lalgudi block, Tiruchirapalli District, Tamil Nadu, India (Fig. 1). The northern part of Lalgudi block has dense dry vegetation and barren lands. The southern part is bounded by River Coleroon. The LalgudiTown is located at the central part of the block. In addition, a comparison was made between surface albedo and NDVI for different land use/cover.

## MATERIALS AND METHODS

### Image selection

Landsat 8 is one of the most recently launched satellite of Landsat series. The Landsat 8 satellite images were downloaded from the USGS Earth Explorer website. To maintain the homogenous dataset, two pairs of images were acquired (December 2014 and January 2015 and December 2017 and January 2018). Paddy is the major crop grown in Lalgudi block during October to January. In order to identify the cultivated lands, the images from December and January were taken in this study. The image acquisition date, solar

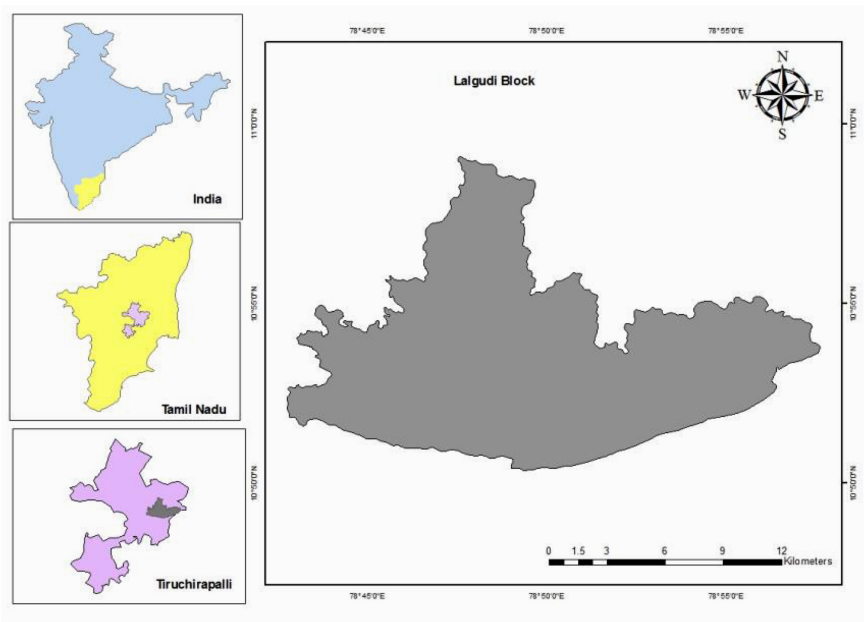


**Fig. 1.** Study area – Lalgudi block of Trichy District.

**Table 1.** Metadata of Landsat 8 images used in this study.

| Sl. No. | Acquisition date (yyyy/mm/dd) | Solar elevation angle (degrees) | Solar azimuth angle (degrees) | Cloud cover in image (%) | Cloud cover in study area (%) |
|---|---|---|---|---|---|
| 1 | 2014-12-05 | 49.38 | 146.60 | 2.46 | 0.77 |
| 2 | 2015-01-22 | 48.22 | 138.31 | 0.01 | 0.00 |
| 3 | 2017-12-29 | 47.08 | 144.18 | 23.15 | 0.40 |
| 4 | 2018-01-30 | 49.39 | 135.62 | 0.17 | 0.00 |

elevation angle and zenith angle for the Landsat 8 data products used in this study is listed in Table 1. The images were selected such that there is no or minimum cloud cover (Table 1) in order to avoid error in classification.

## Computation of surface albedo

Landsat 8 images have eleven bands from which the following six bands were used in albedo estimation i.e. blue (0.45 to 0.51 µm); green (0.53 – 0.59 µm); red (0.64 – 0.67 µm); near infrared (0.85 – 0.88 µm); shortwave infrared (1.57 – 1.65); shortwave infrared (2.11 – 2.29 µm). From the downloaded scenes, different bands were extracted for the study area boundary.

The surface albedo (α) is the ratio of difference between planetary albedo ($\alpha_{toa}$) and atmospheric albedo ($\alpha_{atm}$) of each pixel to the square of atmospheric transmittance (τ).A detailed representation of atmospheric and planetary albedo is depicted in Fig.2. The surface albedo was estimated with the following equation:

$$\alpha = \frac{(\alpha_{toa} - \alpha_{tam})}{\tau^2} \quad (1)$$

The atmospheric transmittance is a function of elevation (Allen *et al.* 1998) and computed using the following equation :

$$\tau = 0.75 + (0.00002 * z) \quad (2)$$

Where z is the elevation raster extracted for the

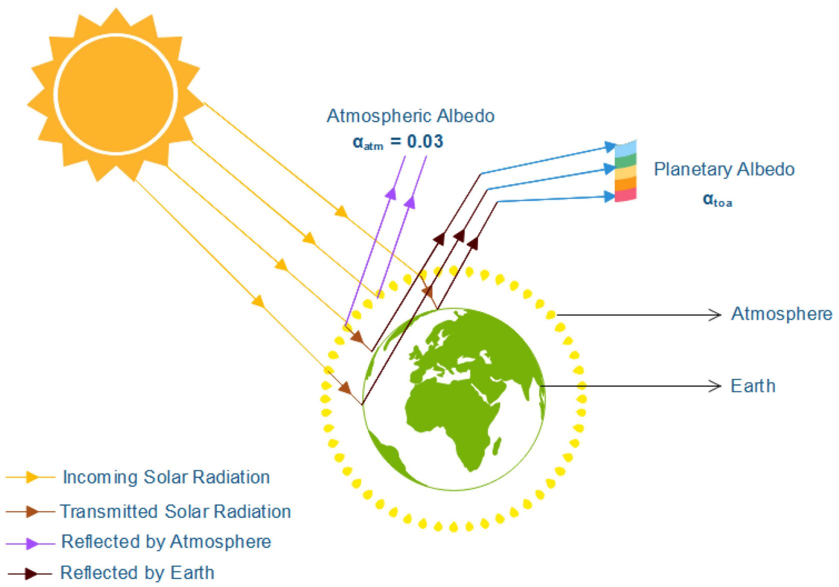


**Fig. 2.** Representation of atmospheric and planetary albedo.

study area from the SRTM DEM. The SRTM DEM was downloaded from USGS Earth Explorer website.

The atmospheric albedo ranges from 0.025 to 0.040. In this study, an average value of 0.03 was taken for atmospheric albedo (Bastianssen *et al.* 1998).

The planetary albedo or albedo without correction was estimated from the six different bands (2, 3, 4, 5, 6, 7) of Landsat8 data set. Firstly, the radiance (ρb) was calculated from the pixel values of different bands (DNb) using the following equation :

$$\rho_b = Add_{rad,b} + (Mult_{rad.b} * DN_b) \quad (3)$$

Where, $Add_{rad,b}$ is additive and $Mult_{rad,b}$ is multiplicative terms related to different band radiance (Table 2). The metadata file downloaded with every scene provides the value of additive and multiplicative terms.

Subsequently, the reflectance of each band was obtained by using the following equation (Chander and Markham 2003):

$$r_b = \frac{[Add_{ref,b} + (Mult_{ref,b} * DN_b)]}{\cos z * d_r} \quad (4)$$

Where, $Add_{ref,b}$ is additive and $Mult_{ref,b}$ is multiplicative terms related to different band reflectance given in metadata file (Table 3). The angle z is called sun zenith angle which is 90 minus sun elevation angle provided in metadata file of each scene (Table 1). $d_r$ corresponds to correction of eccentricity of the terrestrial orbit and the equation is as follow as :

$$d_r = \left(\frac{1}{d_{ES}}\right)^2 \quad (5)$$

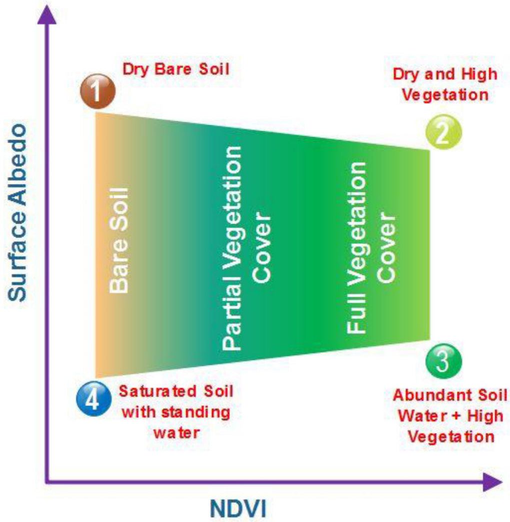


**Fig. 3.** Surface albedo-NDVI variation with soil, water and plant.

Where, $d_{ES}$ is the Earth-to-Sun distance in astronomic unit (AU) for each selected days (Table 2).

It is important to determine the solar constant Kb, (W m$^{-2}$ μm) for each bands and $K_b$ was determined with the following equation :

$$K_b = \frac{\pi * \rho_b}{r_b \cos z * d_r} \quad (6)$$

Where, all the terms were estimated in previous steps for different bands. The albedo weights $P_b$ were obtained by using the following expression :

**Table 2.** Multiplicative and additive factors used in radiance calculation.

| Date | 2014-12-05 | | 2015-01-22 | | 2017-12-29 | | 2018-01-30 | |
|---|---|---|---|---|---|---|---|---|
| Band | $Mult_{rad}$ | $Add_{rad}$ | $Mult_{rad}$ | $Add_{rad}$ | $Mult_{rad}$ | $Add_{rad}$ | $Mult_{rad}$ | $Add_{rad}$ |
| 2 | 1.32E-02 | -66.1932 | 1.33E-02 | -66.3701 | 1.33E-02 | -66.4792 | 1.33E-02 | -66.2511 |
| 3 | 1.22E-02 | -60.9965 | 1.22E-02 | -61.1595 | 1.23E-02 | -61.2600 | 1.22E-02 | -61.0498 |
| 4 | 1.03E-02 | -51.4356 | 1.03E-02 | -51.5731 | 1.03E-02 | -51.6579 | 1.03E-02 | -51.4807 |
| 5 | 6.30E-03 | -31.4761 | 6.31E-03 | -31.5602 | 6.32E-03 | -31.6121 | 6.30E-03 | -31.5036 |
| 6 | 1.57E-03 | -7.82781 | 1.57E-03 | -7.8487 | 1.57E-03 | -7.8616 | 1.57E-03 | -7.8346 |
| 7 | 5.28E-04 | -2.63839 | 5.29E-04 | -2.6454 | 5.30E-04 | -2.6497 | 5.28E-04 | -2.6407 |

**Table 3.** Variables used in albedo calculation.

| Acquisition date (yyyy/mm/dd) | Solar zenith angle (degrees) | $Mult_{ref}$ | $Add_{ref}$ | $d_{ES}$ |
|---|---|---|---|---|
| 2014-12-05 | 40.62 | 0.00002 | -0.1 | 0.98549 |
| 2015-01-22 | 41.77 | 0.00002 | -0.1 | 0.98417 |
| 2017-12-29 | 42.92 | 0.00002 | -0.1 | 0.98336 |
| 2018-01-30 | 40.61 | 0.00002 | -0.1 | 0.98505 |

$$P_b = \frac{K_b}{K_{sum}} \qquad (7)$$

Where, $K_{sum}$ is the sum of $K_b$ values of different bands used in calculation. Finally, the planetary albedo was estimated as the sum of product of albedo weight and reflectance of different bands used in the calculation. The expression for determining planetary albedo is as follow as:

$$\alpha_{toa} = \sum_{b-2}^{7} p_i * r_i \qquad (8)$$

By substituting in Eq. (1), the surface albedo raster was obtained. The calculations were done using Raster Calculator tool in ArcGIS.

## Computation of normalized difference vegetation index

NDVI is the ratio of difference between reflectivity of near-infrared (NIR) band and red band to their sum. The expression for estimation of NDVI is as follow as:

$$NDVI = \frac{NIR - RED}{NIR + RED}$$

In Landsat 8 image, near infrared is band 5 and the red is band 4. Using Raster Calculator tool in Arc-GIS, NDVI raster were obtained.

## Comparison of surface albedo-NDVI for land use/cover classification

The combination of Surface Albedo-NDVI helps in identification of vegetation cover changes (Yao *et al.* 2008). The variation of surface albedo and NDVI for different surfaces is described in Fig. 3. A dry bare soil has high reflection and less NDVI (point 1); dry land with high vegetation has high albedo and high NDVI (point 2); high vegetation with soil water content has low albedo and high NDVI (point 3) and soil with ample moisture content or standing water like paddy fields or water bodies have less albedo and less NDVI (point 4).

Using band statistics tool, minimum, maximum, mean and standard deviation of surface albedo and NDVI raster were calculated.Subsequently, the correlation between these two parameters was determined. The surface albedo and NDVI were compared for different land use/cover in the study area. The ground control points were taken by surveying the entire block.

## RESULTS AND DISCUSSION

The spatial and temporal variation of surface albedo (Fig.4) and NDVI (Fig. 5) of the study area were obtained for the four selected scenes.The minimum, maximum, mean, standard deviation and correlation coefficient for Surface Albedo-NDVI is presented in Table 3. In the scenes taken on 05-12-2014 and 29-12-2017, the maximum surface albedo values (0.7490 and 0.8397) was due to presence of clouds. Oke (1987) also reported surface albedo values of clouds ranges from 0.6 to 0.9.

The surface albedo values obtained in the south-eastern part of the study area ranges from 0.20 to 0.37. This indicates the presence of dry sand of River Coleroon. Similarly the surface albedo values of south-western part varied from 0.05 to 0.10 which indicates the standing water in the flow path of River Coleroon. The values obtained were consistent with those values reported in literature for surface albedo of sand (0.4) and water (0.03) (Oke1987).

**Table 4.** Albedo and NDVI band statistics for different image acquisition dates.

| Acquisition date (yyyy/mm/dd) | Index | Minimum | Maximum | Mean | Standard deviation | Correlation coefficient |
|---|---|---|---|---|---|---|
| 2014-12-05 | Albedo | 0.0650 | 0.7490 | 0.1666 | 0.0333 | -0.03 |
| | NDVI | -0.0788 | 0.5374 | 0.3167 | 0.1048 | |
| 2015-01-22 | Albedo | 0.0495 | 0.3891 | 0.1538 | 0.0302 | -0.34 |
| | NDVI | -0.0969 | 0.5320 | 0.3159 | 0.0872 | |
| 2017-12-29 | Albedo | 0.0707 | 0.8397 | 0.1561 | 0.0299 | -0.39 |
| | NDVI | -0.0795 | 0.5373 | 0.3258 | 0.0965 | |
| 2018-01-30 | Albedo | 0.0584 | 0.3768 | 0.1556 | 0.0291 | -0.43 |
| | NDVI | -0.0795 | 0.5373 | 0.3258 | 0.0965 | |

The surface albedo for barren land and lush vegetation present in northern part ranges from 0.2 to 0.3 and 0.12 to 0.23 respectively. Allen *et al*. (1998) also reported average albedo values for vegetation as 0.23. The central part of Lalgudi has cultivated lands especially paddy fields. The surface albedo in central part clearly indicates stagnant water in the paddy fields in December 2014 and January 2018 images and the soil covered with vegetation in January 2015 and December 2017 images. The settlements and

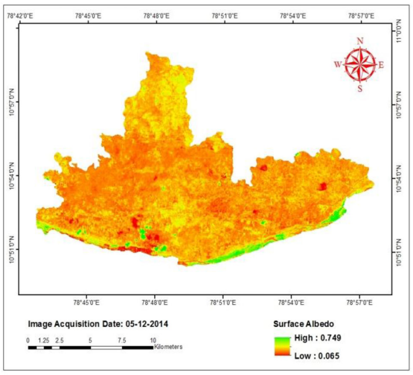


**(a) Surface albedo – Dec 2014**

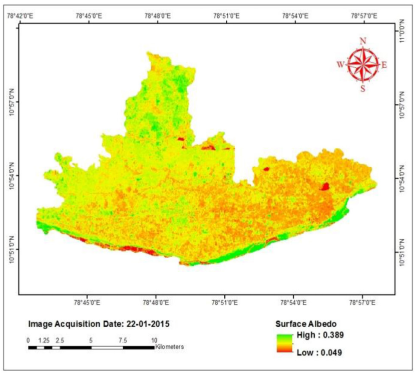


**(b) Surface albedo – Jan 2015**

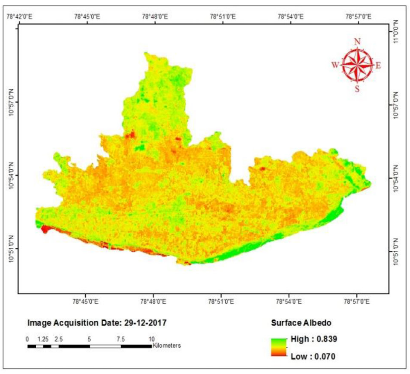


**(c) Surface Albedo – Dec 2017**

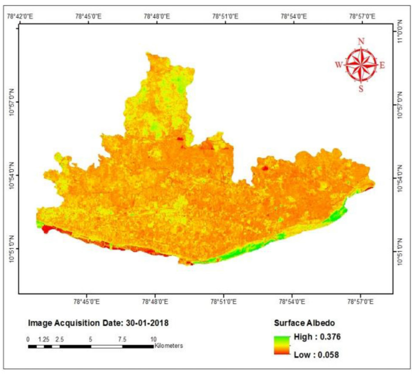


**(d) Surface Albedo – Jan 2018**

**Fig. 4.** Spatial and temporal changes of surface albedo in Lalgudi block.

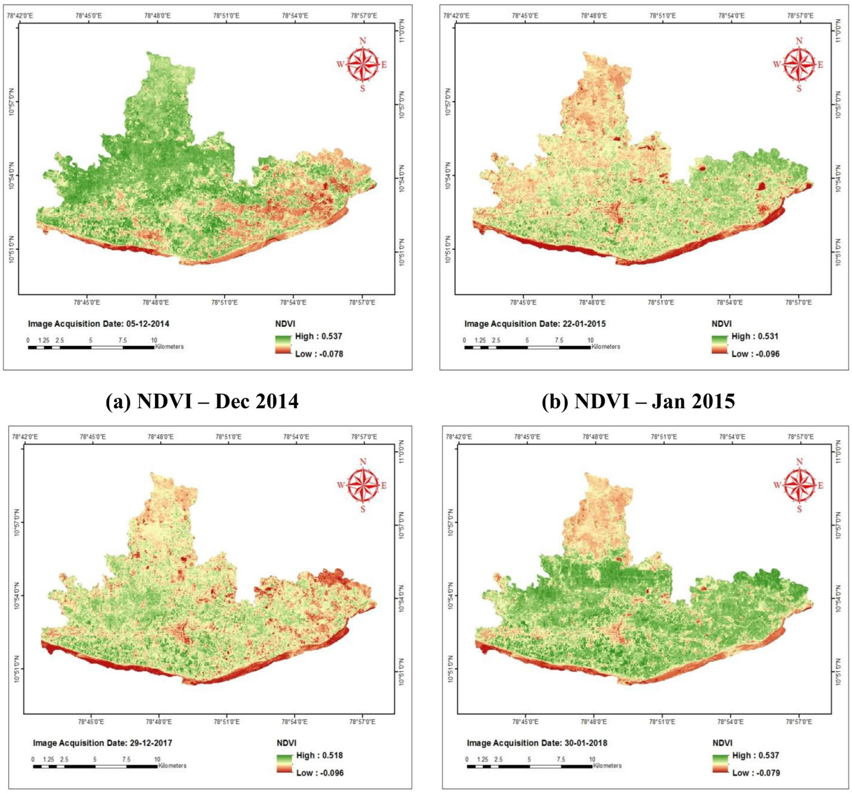


**(a) NDVI – Dec 2014** **(b) NDVI – Jan 2015**

**(c) NDVI – Dec 2017** **(d) NDVI – Jan 2018**

**Fig. 5.** Spatial and temporal changes of NDVI in Lalgudi block.

buildings is clearly demarcated in the central part of the town with surface albedo values ranging from 0.15 to 0.20 (Oke 1988, Spångmyr 2010).

The negative values (-0.07 to -0.09) of NDVI obtained in southern part of Lalgudi block indicates the presence of a water body that is River Coleroon. The NDVI values fails to differentiate the stagnant water and sand bed as compared to albedo values for the River Coleroon. The estimated NDVI for the settlements present in inner part of the study area ranges from 0.1 to 0.3. Subsequently, the NDVI for vegetation ranges from 0.3 to 0.5. Salifu and Agyare (2012) also reported NDVI values for water bodies, cultivated lands and settlements as -0.06, 0.31 and 0.27 respectively. The presence of patches of clouds is also not clear in NDVI maps.

The correlation coefficient obtained between surface albedo and NDVI for the four selected scenes is given in Table 4. The negative value indicates that for any surface, NDVI and surface albedo values varies inversely. If albedo increases then NDVI decreases (Yao *et al.* 2008).

The ground control points were taken at different land use/cover. A comparison was made between the surface albedo and NDVI values those ground control points. Figs. 6a–6d depicts the surface albedo and NDVI comparison for different land use/cover. The existence of water in the lake during December 2014 and January 2015 is clearly indicated by low NDVI and surface albedo values. This is because of water having lesser reflectivity and being colorless. Subsequently, in December 2017 and January 2018 images, the higher values of surface albedo and NDVI for lake, indicates the presence of algal blooms covering the water surface. This kind of algal growth indicates the eutrophication of lake which is due

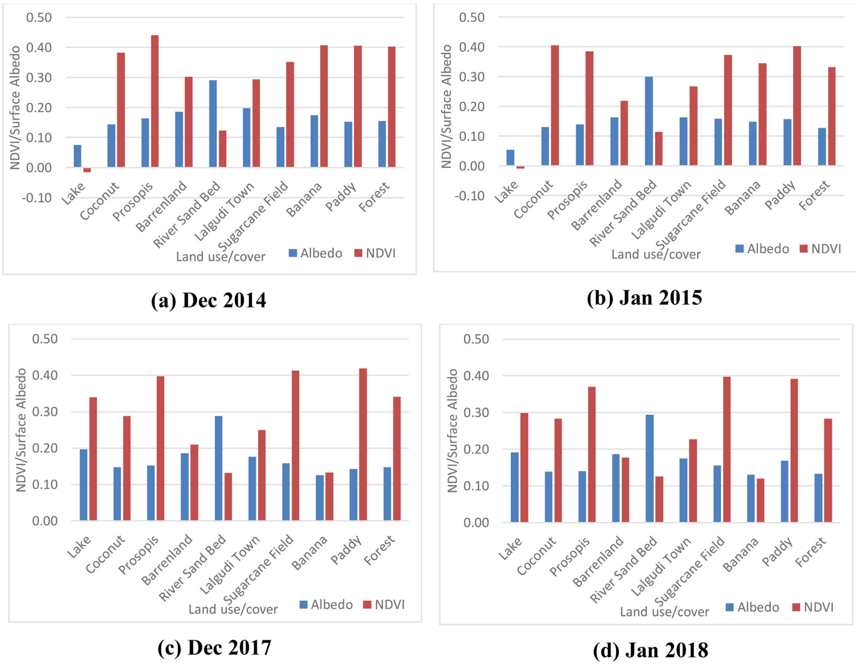


**Fig. 6.** Surface albedo-NDVI variation for different land use/cover.

the excess use of fertilizer and domestic activities happening around lake. Coconut and banana fields exhibit similar trends of surface albedo and NDVI values (Figs. 6a, 6b). The drop in NDVI and surface albedo of banana in Figs. 6c, 6d is because of new banana plants have been planted in the same field. Prosopis and forest areas exhibit similar trend in all the images. When December 2017 and December 2018 image is examined closely for sugarcane (Figs. 6c, 6d), there is a drop in NDVI values. This is due to paling of green leaves and also it indicates the harvest of sugarcane crop. The location selected for paddy is at the stage of maturity stage with good green cover and hence high values of NDVI is noted. Lalgudi town shows same trend in all the images. This comparison aids in identification of different land use/cover by examining the nature of trends exhibited.

## CONCLUSION

In this study, Landsat 8 satellite images acquired from the USGS Earth Explorer website was used for calculation of surface albedo and NDVI. Surface albedo and NDVI were calculated for two pairs of images (December 2014 and January 2015 and December 2017 and January 2018). The comparison of surface albedo-NDVI showed negative correlation coefficient which indicates the inverse relationship between albedo and NDVI. The surface albedo gave a clear indication of sand, water, settlements and cultivated land whereas NDVI distinguished the cultivated areas significantly. This kind of comparisons brings out a good differentiation in different land use/cover and helps in preparation of spatial and temporal land use/cover maps.

## REFERENCES

Allen RG, Pereira LS, Raes D, Smith M (1998) "Crop evapo-transpiration: Guidelines for computing crop water requirements." Food and Agricultural Organization, Rome.

Bastiaanssen WGM, Menenti M, Feddes RA, Holslag AAMA (1998) Remote Sensing surface energy balance algorithm for Land (SEBAL) – Formulation. *J Hydrol,* pp 198—212.

Chander G, Markham B (2003) Revised Landsat 5 – TM radio metric calibration procedures and post calibration dynamic-ranges. *IEEE Transactions on Geosci and Rem Sens* 41:2674—2677.

da Silva BB, Braga AC, Braga CC, de Oliveira LLM, Montenegro SMGL, Junior BB (2016) Procedures for calculation of the albedo with OLI-Landsat 8 images: Application to the Brazilian semi-arid. *Revista Brasileira de Engenharia Agrícola e Ambienta* l 20 (1) : 3—8.

Liaqat UW, Choi M (2015) Surface energy fluxes in the Northeast Asia ecosystem: SEBS and METRIC models using Landsat satellite images. *Agric For Meteorol* 214-215 : 60—79.

Oke TR (1987) Boundary Layer Climates. 2nd edn. Methuen, London, England and New York, NY, USA, pp 452.

Oke TR (1988)The urban energy balance. Progress in Physical Geography. Edward Arnold Publishers LTD, London, England, pp 12 (1) : In press.

Roy DP, Wulder MA, Loveland TR, Woodcock CE, Allen RG, Anderson MC, Helder D, Irons JR, Johnson DM, Kennedy R, Scambos TA, Schaaf CB, Schott JR, Sheng Y, Vermote EF, Belward AS, Bindschadler R, Cohen WB, Gao F, Hipple JD, Hostert P, Huntington J, Justice CO, Kilic A, Kovalskyy V, Lee ZP, Lymburner L, Masek JG, McCorkel J, Shuai Y, Trezza R, Vogelmann J, Wynne RH, Zhu Z (2014) Landsat-8: Science and product vision for terrestrial global change research. *Rem Sens Environ* 145:154–172.

Salifu T, Agyare WA (2012) Distinguishing land use types using surface albedo and normalized vegetative index derived from the SEBAL model for the Atankwidi and Aframsub-catch ments in Ghana. *ARPN J Engg Appl Sci* 7 (1) : 69—80.

Semmens KA, Anderson MC, Kustas WP, Gao F, Alfieri JG, McKee L, Prueger JH, Hain CR, Cammalleri C, Yang Y, Xia T, Sanchez L, Alsina MM,Vélez M (2016) Monitoring daily evapotranspiration over two California vineyards using Landsat 8 in a multi-sensor data fusion approach. *Rem Sens* Environ 185 :155—170.

Spångmyr M (2010) Global effects of albedo change due to urbanization. Department of Earth and Ecosystem Sciences. Division of Physical Geography and Ecosystems Analysis. Lund University. Sweden. Seminar series No., pp 180.

Yao Y, Qin Q, Zhu L, Yang N (2008) Relating Surface Albedo and Vegetation Index with Surface Dryness using Landsat ETM+ Imagery. *IGARSS I*, pp 312-315.